Supporting Information

The nature of the styrylindolium dye: transformations among monomer, aggregates and water adducts

Chang Liu,[a] Yan Lu, [a] Song He, [a] Qing Wang, [a] Liancheng Zhao, [a,b] and Xianshun Zeng*[a]

† *Key Laboratory of Display Materials & Photoelectric Devices, Ministry of Education, School of Materials Science & Engineering, Tianjin University of Technology, Tianjin 300384, China. Fax: +86-22-60215226; Tel: +86-22-60216748; E-mail: xshzeng@tjut.edu.cn*

‡ *School of Materials Science and Engineering, Harbin Institute of Technology, Harbin 150001, China*.

Materials and methods: All solvents and reagents (analytical grade) were obtained commercially and used as received unless otherwise mentioned. NMR spectra were recorded on a Bruker spectrometer at 400 (^{1}H NMR) MHz, 100 (^{13}C NMR) MHz. Chemical shifts (δ values) were reported in ppm down field from internal Me_4Si (^{1}H and ^{13}C NMR). High resolute ESI mass spectra were recorded on a Xevo QTof mass spectrometer (Waters, USA). Elemental analyses were performed on a Vanio-EL elemental analyzer (Analysensysteme GmbH, Germany). UV absorption spectra were recorded on a UV-3600 UV-VIS spectrophotometer (Shimadzu, Japan). Fluorescence measurements were performed using an F-4600 fluorescence spectrophotometer (Hitachi, Japan) equipped with a quartz cell (1 cm × 1 cm). Melting points were recorded on a Boetius Block apparatus and are uncorrected.

Synthesis of tetrafluoroborate of 2-{2-[2-methoxyphenyl]ethenyl}-1,3,3'-trimethylindoline 4. To a 50 ml flask, was charged N-methyl-2,3,3'-trimethylindolium iodide **1** (650 mg, 2.0 mmol), 2-methoxylbenzenaldehyde **2** (360 mg, 2.6 mmol) and anhydrous ethanol (25 mL). The reaction mixture was washed with nitrogen flow for 30 min to remove oxygen, and then stirred at 90 ^{o}C for 24 h in dark to afforded compound **3**. After cooling to room temperature, KBF_4 (410 mg, 3.3 mmol) was added in one portion to the reaction mixture. The suspension was refluxed for another 2 h in dark. The solvent was removed under reduced pressure. The residue was dissolved in DMF (5 mL) and filtered; the solid salt was washed with DMF (2 × 1 mL). The filtrate was condensed to dryness under reduced pressure. The residue was dissolved with

hot ethanol (10 mL). After cooling to room temperature, **4** was crystallized from the solvent to get pure product (570 mg) in 72% yield; mp 212-214 ^{o}C; HRMS: m/z $[M\text{-}BF_4^-]^+$ = 292.1696; ^{1}H NMR ($CDCl_3$, 400 MHz, ppm): 1.87 (s, 6H), 4.03 (s, 3H), 4.47 (s, 3H), 7.00 (d, *J* = 8.4 Hz, 7.19 (t, *J* = 7.6 Hz, 1H), 7.60-7.58 (t, *J* = 5 Hz, 4H), 7.70 (d, *J* = 7.2 Hz, 1H), 7.85 (d, *J* = 16.4 Hz, 1H), 8.38 (d, *J* = 8 Hz, 1H), 8.62 (d, *J* = 16.4 Hz, 1H) (Figure S23); ^{13}C NMR (DMSO-d_6, 100 MHz, ppm): 182.7, 160.32, 148.16, 144.15, 142.71, 136.35, 131.13, 130.22, 129.89, 123.74, 123.45, 122.03, 116.12, 114.13, 113.27, 57.32, 52.90, 35.54, 26.75 (Figure S9). Elemental analysis calcd (%) for $C_{20}H_{22}B_2F_4NO\bullet0.5CH_2Cl_2$: C, 58.39; H, 5.50, N, 3.32; Found: C, 58.71; H, 5.66; N, 3.32.

Table S1. Temperature Dependence of the Equilibrium Constant (K) for the Thermal Interconversion of **4** to **4-OH**.

T (K)	288	293	298	303	308	313	318	323
K	1.0038	1.0046	1.0054	1.0068	1.0082	1.0097	1.0117	1.0137

Table S2. Temperature Dependence of the Equilibrium Constant (K) for the Thermal Interconversion of the D-Aggregate of **4** to its Monomer.

T (K)	288	293	298	303	308	313	318	323
K	1.0142	1.0175	1.0222	1.02734	1.03312	1.0398	1.0478	1.0557

The temperature-dependent fluorescence change could be expressed thermodynamically by a D-aggregate-monomer equilibrium model. The equilibrium constant *K* for the equilibrium between D-aggregate and **4** in eqn. (S1) can be analysed by eqn. (S2), where $I_{\text{lower temp.}}$, $I_{\text{higher temp.}}$ and I_{obs} denote the fluorescence intensity at λ_{em} for the lower-temperature and higher-temperature species and the experimental fluorescence intensity, respectively. The temperature dependence of the equilibrium constant *K* is given by eqn. (S3), where *R* and *T* are the gas constant and absolute temperature, respectively. The temperature dependence of *K* is summarized in Table S2. The least squares fit for eqn. (S3) has been carried out using the postulated values of $I_{\text{lower temp.}}$ and $I_{\text{higher temp}}$ until a good linear relationship in the ln *K vs.* T^{-1} plot could be obtained. An optimized linear plot of ln *K* for **4** against T^{-1} could be obtained as shown in Inset of Fig. 7b on the assumption that $I_{\text{lower temp}}$ and $I_{\text{higher temp}}$ are equal to 667 at 273 K and 281 at 338 K, respectively.

$$\textbf{D-aggr.}_{\text{ lower temp.}} \underset{}{\overset{K}{\rightleftharpoons}} \textbf{4}_{\text{ higher temp.}} \qquad \text{(S1)}$$

$$K = \frac{[\textbf{4}_{\text{ higher temp.}}]}{[\textbf{D-aggr.}_{\text{ lower temp.}}]} = \frac{(I_{\text{lower temp.}} - I_{\text{obs}})}{(I_{\text{obs}} - I_{\text{higher temp.}})} \qquad \text{(S2)}$$

$$\ln K = \ln \frac{(I_{\text{lower temp.}} - I_{\text{obs}})}{(I_{\text{obs}} - I_{\text{higher temp.}})} = \frac{\Delta S^{o}}{R} - \frac{\Delta H^{o}}{RT} \qquad \text{(S3)}$$

From the slope ($-\Delta H^{o}/R$) of the van't Hoff plot a standard enthalpy ΔH^{o} value of +887.82 J/mol was calculated. From this value and the K value of 1.0222 at 25 ^{o}C, a standard entropy ΔS^{o} value of +3.16 $J \cdot mol^{-1} \cdot K^{-1}$ was determined.

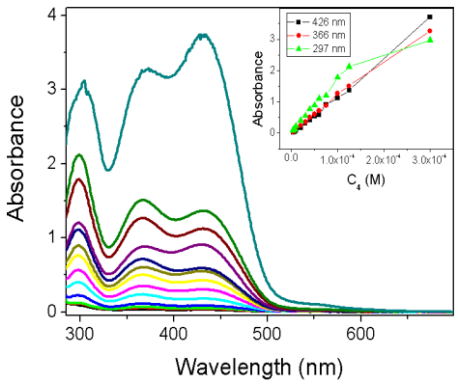

Figure S1. Concentration-dependent UV/Vis absorption spectra of **4** in toluene from 3.5×10^{-6} M to 3×10^{-4} M. Inset: Plot of the absorptions of H-aggregate at 297 nm, D-aggregate at 366 nm and monomer at 426 nm against concentration.

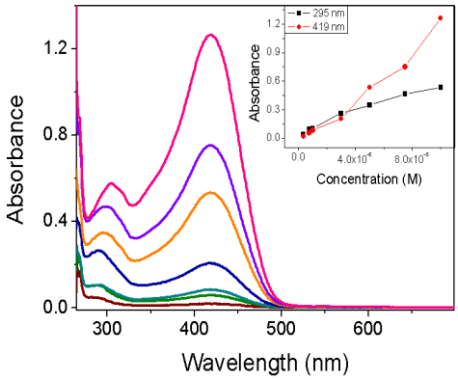

Figure S2. Concentration-dependent UV/Vis absorption spectra of **4** in DMF from 3.5×10^{-6} M to 1×10^{-4} M. Inset: Plot of the absorptions of H-aggregate at 295 nm and monomer at 419 nm against concentration.

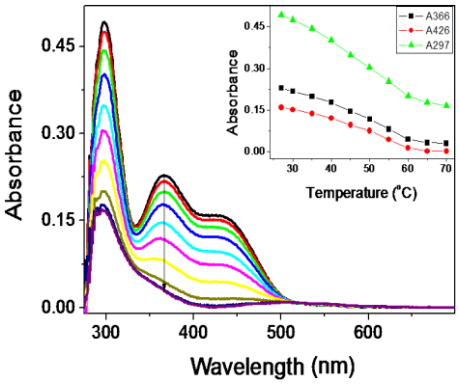

Figure S3. Temperature-dependent transformation from the monomer, D-aggregate and H-aggregate to water adducts for dye **4** (3×10^{-5} M) in equilibrated toluene (the solution of **4** was stocked for 3.5 h before the experiments). Inset: plot of the absorption intensity changes at 426 nm, 366 nm and 297 nm against temperature.

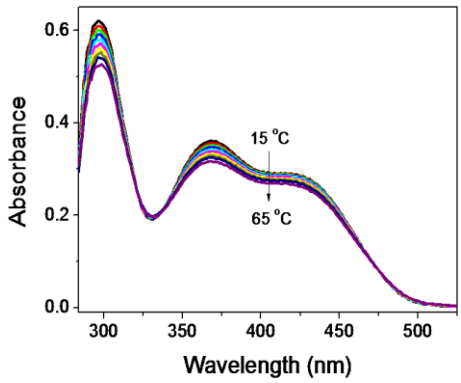

Figure S4. Temperature-dependent transformation from monomer, D-aggregate and H-aggregate to water adducts for dye **4** (3×10^{-5} M) in THF equilibrated for 3.5 h before the experiments.

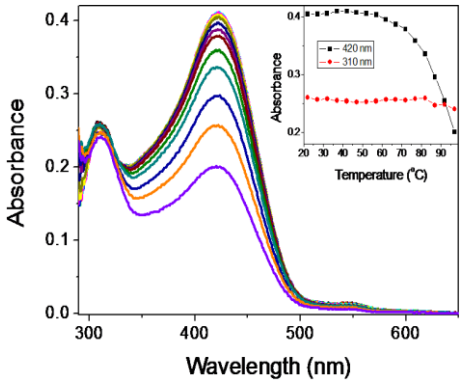

Figure S5. Temperature-dependent transformation from monomer, D-aggregate and H-aggregate to water adducts for dye **4** (3×10^{-5} M) in equilibrated THF/H_2O (v/v, 3:1) solution. Inset: Plot of the absorption of H-aggregate at 310 nm and monomer at 420 nm against temperature. Note: the solution of **4** was equilibrated for 17 h before the experiments.

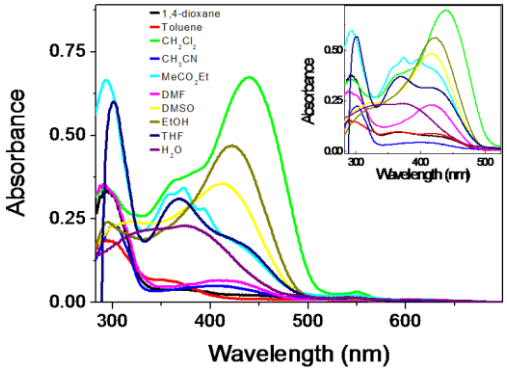

Figure S6. The absorption spectra of **4** (3×10^{-5} M) equilibrated for 60 h in various solvents before experiments. Inset: The absorption spectra of 4 upon the addition of acetic acid in various solvents. Note: The spectra were recorded immediately upon the addition of acetic acid. The line was presented in the same colour for the equilibrated solutions and the addition of acetic acid.

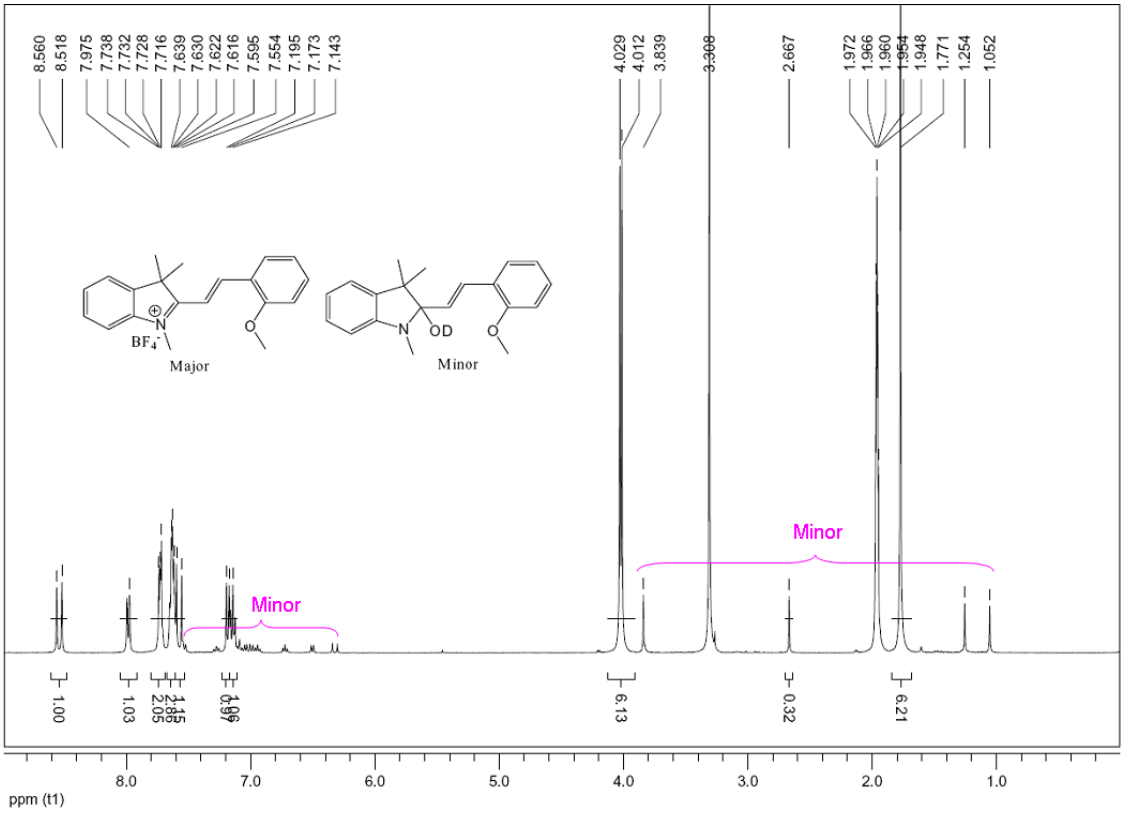

Figure S7. ^{1}H NMR of **4** (400 MHz) in CD_3CN. The spectra of the freshly prepared solution of **4** were taken within 10 min. Two species can be observed in the spectra (about 10% of water adduct can be observed as marked 'Minor' in the spectra), indicated the formation of water adducts by the reaction of **4** with the water residue in the solvent carried out quickly.

^{1}H NMR (CD_3CN, 400 MHz, ppm): 8.54 (d, 1H, *J* = 16.4 Hz), 7.98 (d, 1H, *J* = 7.6 Hz), 7.74-7.71 (m, 2H), 7.65-7.61 (m, 3H), 7.57 (d, 1H, *J* = 16.4 Hz), 7.18 (d, 1H, *J* = 8.4 Hz), 7.14 (t, 1H, *J* = 7.6 Hz), 4.03 (s, 3H), 4.01 (s, 3H), 1.77 (s, 6H). At the same time, about 10% of water adduct can be observed at 7.53 (d, 1H, *J* = 7.6 Hz), 7.28 (d, 1H, *J* = 7.2 Hz), 7.12 (1H, overlapped), 7.09 (t, 1H, *J* = 8.0 Hz), 7.04 (d, 1H, *J* = 7.2 Hz), 6.99 (d, 1H, *J* = 8.0 Hz), 6.94 (t, 1H, *J* = 7.6 Hz), 6.72 (t, 1H, *J* = 7.6 Hz), 6.50 (d, 1H, *J* = 7.6 Hz), 6.32 (d, 1H, *J* = 16.4 Hz), 3.84 (s, 3H), 2.67 (s, 3H), 1.25 (s, 3H), 1.05 (s, 3H), respectively.

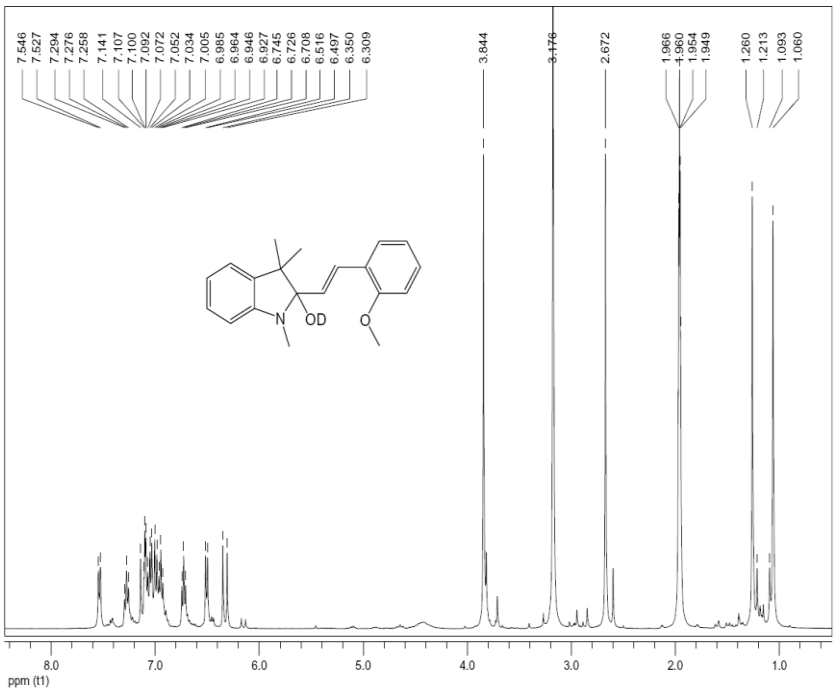

Figure S8. ^{1}H NMR of **4** (400 MHz, CD_3CN) upon the addition of NaOD (2 equivalents). The spectra were recorded immediately after the addition of NaOD.

^{1}H NMR (CD_3CN, 400 MHz, ppm): 7.53 (d, 1H, *J* = 7.6 Hz), 7.28 (d, 1H, *J* = 7.2 Hz), 7.12 (d, 1H, *J* = 16.4 Hz), 7.09 (t, 1H, *J* = 8.0 Hz), 7.04 (d, 1H, *J* = 7.2 Hz), 6.99 (d, 1H, *J* = 8.0 Hz), 6.95 (t, 1H, *J* = 7.6 Hz), 6.73 (t, 1H, *J* = 7.6 Hz), 6.50 (d, 1H, *J* = 7.6 Hz), 6.33 (d, 1H, *J* = 16.4 Hz), 3.84 (s, 3H), 2.67 (s, 3H), 1.26 (s, 3H), 1.06 (s, 3H).

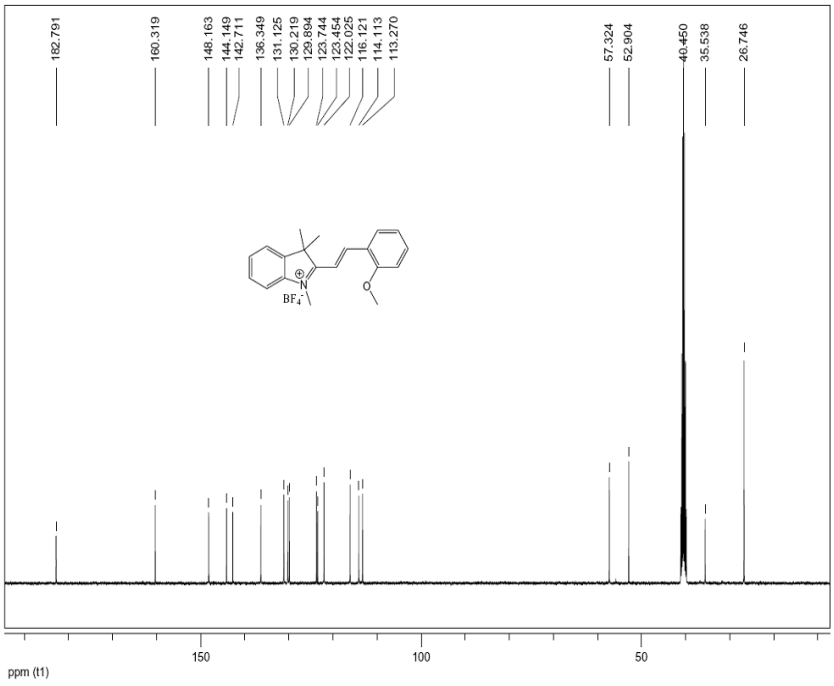

Figure S9. ^{13}C NMR of **4** (100 MHz) in DMSO-d_6.

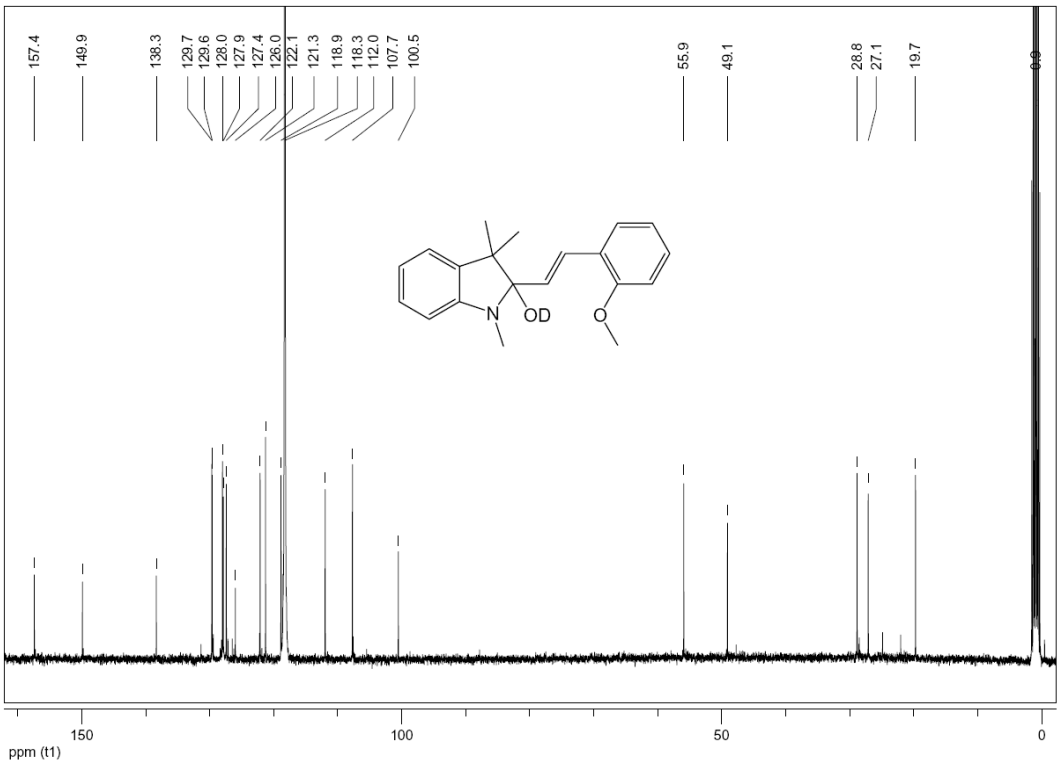

Figure S10. ^{13}C NMR of **4** (100 MHz) in CD_3CN

^{13}C NMR (CD_3CN, 100 MHz, ppm): 157.4, 149.9, 138.3, 129.7, 129.6, 128.0, 127.9, 127.4, 126.0, 122.1, 121.3, 118.9, 112.0, 107.7, 100.5, 55.9, 49.1, 28.8, 27.1, 19.7.

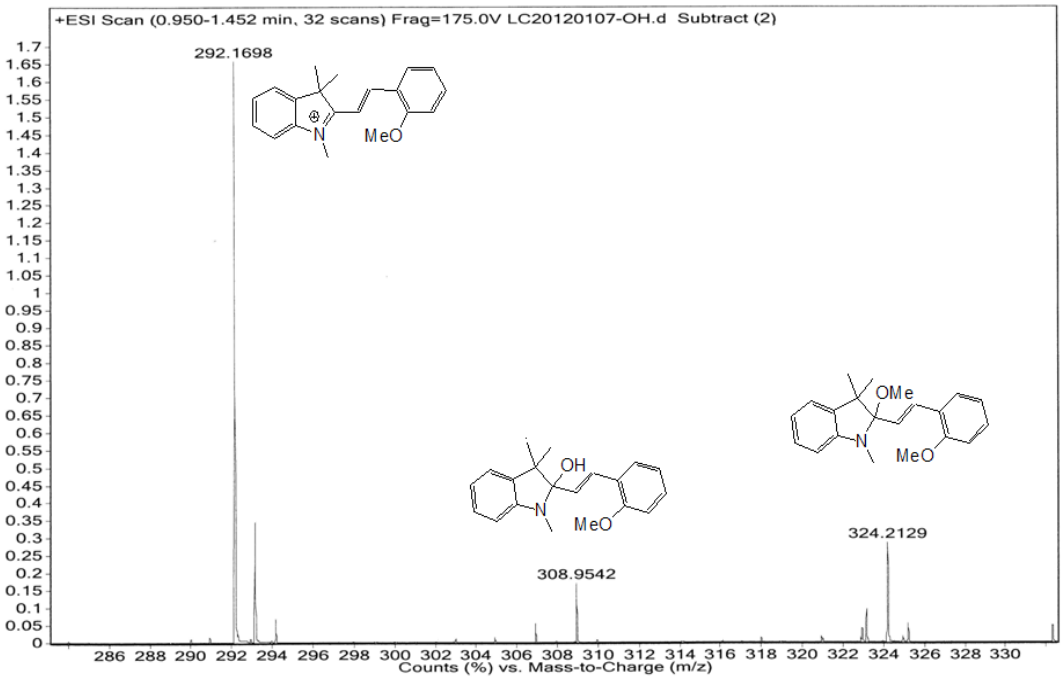

Figure S11. High-resolution mass spectra (HRMS) of **4** in an equilibrated methanol/H_2O (99:1, v/v) solution. The peak (m/z) at 308.9542 and the peak (m/z) at 324.2129 corresponded the water adducts and the methanol adducts, respectively.

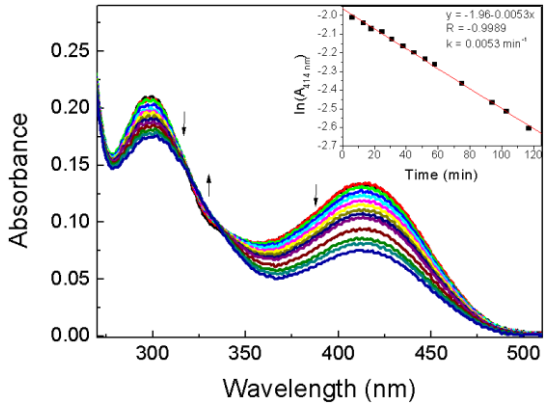

Figure S12. The kinetic measurements of the reaction of **4** (30 μM) with water in NaOH (0.01 M) under pseudo-first-order conditions by UV/Vis absorption spectra. Inset: plot of $\ln(A_{414\,nm})$ at 414 nm observed against time (min) from the reaction between **4** (30 μM) and H_2O in NaOH (0.01 M) at T = 298 K. The red line overlaid on the experimental data points is theoretical fit generated using $k_{obs} = 5.3 \times 10^{-3}$ min^{-1}.

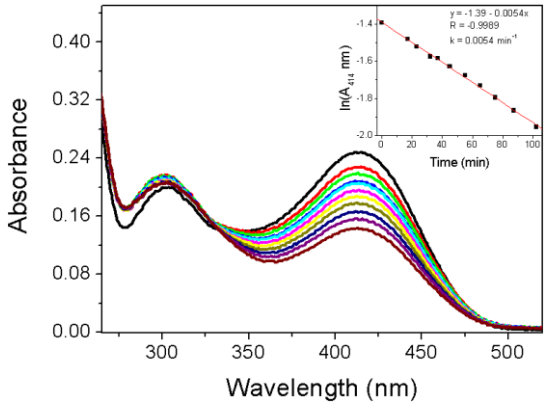

Figure S13. The kinetic measurements of the reaction of **4** (30 μM) with water in NaOH (0.005 M) under pseudo-first-order conditions by UV/Vis absorption spectra. Inset: plot of $\ln(A_{414\,nm})$ at 414 nm observed against time (min) from the reaction between **4** (30 μM) and H_2O in NaOH (0.005 M) at T = 298 K. The red line overlaid on the experimental data points is theoretical fit generated using $k_{obs} = 5.4 \times 10^{-3}$ min^{-1}.

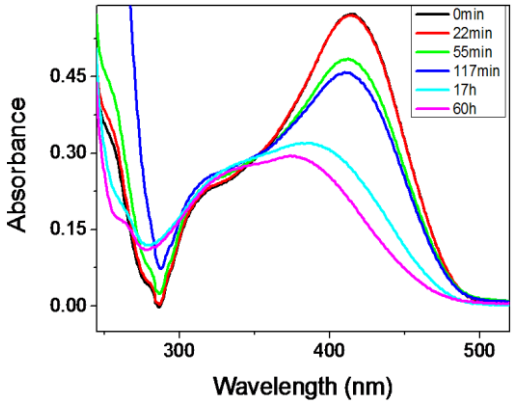

Figure S14. Time-dependent transition from monomer into the D-aggregate for dye **4** (3×10^{-5} M) in 1.5 M HCl at 25 ^{o}C.

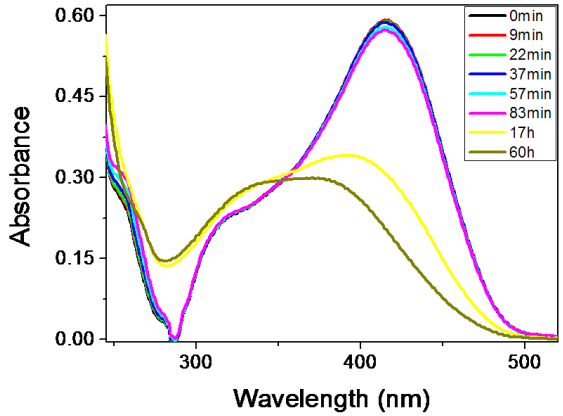

Figure S15. Time-dependent transition from monomer into D-aggregate for dye **4** (3×10^{-5} M) in 2.1 M HCl at 25 ^{o}C.

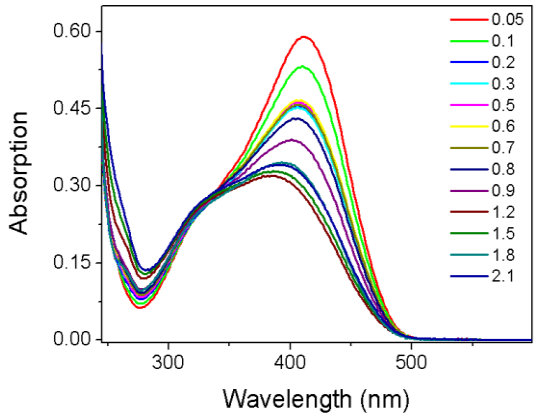

Figure S16. UV/Vis spectra of **4** (3×10^{-5} M) equilibrated for 17 h in different concentrations of HCl (from 0.05 M to 2.1 M) at 25 ^{o}C. The monomeric absorptions at ca. 410 nm of all the equilibrated solutions decreased with the increased HCl concentrations from 0.05 M to 1.2 M. At the same time, the D-aggregate absorptions at ca. 330 nm increased slightly with the increased HCl concentrations from 0.05 M to 1.2 M. However, the absorptions at 410 nm slightly increased with higher HCl concentrations than 1.2 M.

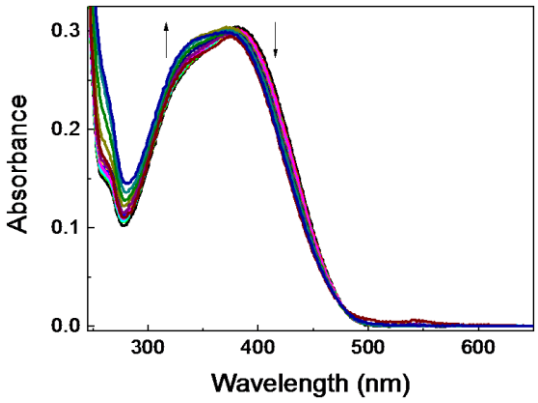

Figure S17. UV/vis apectra of **4** (3×10^{-5} M) in different of HCl concentrations (from 0.05 M to 2.1 M) equilibrated for 60 h at 25 ^{o}C. The monomeric absorptions at ca. 410 nm slightly decreased with the increased HCl concentrations from 0.05 M to 1.2 M. At the same time, the D-aggregate absorptions at ca. 330 nm increased slightly with the increased HCl concentrations from 0.05 M to 1.2 M. The absorptions at 330 nm and the absorptions at 410 nm kept constant while the HCl concentrations higher than 1.2 M.

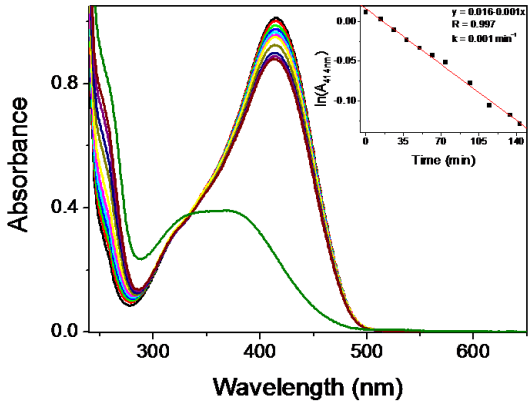

Figure S18. The kinetic measurements of the formation of D-aggregate in HCl (1.2 M) under pseudo-first-order conditions by UV/Vis absorption spectra. Inset: plot of $\ln(A_{414\ nm})$ at 414 nm observed against time (min) from the reaction between **4** (30 μM) and H_2O in NaOH (0.005 M) at T = 298 K. The red line overlaid on the experimental data points is theoretical fit generated using k_{obs} = 1.0 × 10^{-3} min^{-1}.

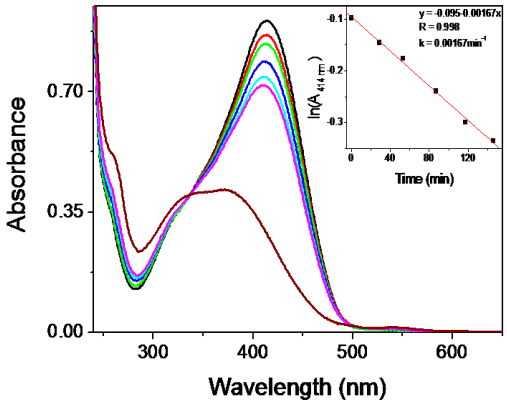

Figure S19. The kinetic measurements of the formation of D-aggregate in HCl (1.5 M) under pseudo-first-order conditions by UV/Vis absorption spectra. Inset: plot of $\ln(A_{414\ nm})$ at 414 nm observed against time (min) from the reaction between **4** (30 μM) and H_2O in NaOH (0.005 M) at T = 298 K. The red line overlaid on the experimental data points is theoretical fit generated using k_{obs} = 1.67 × 10^{-3} min^{-1}.

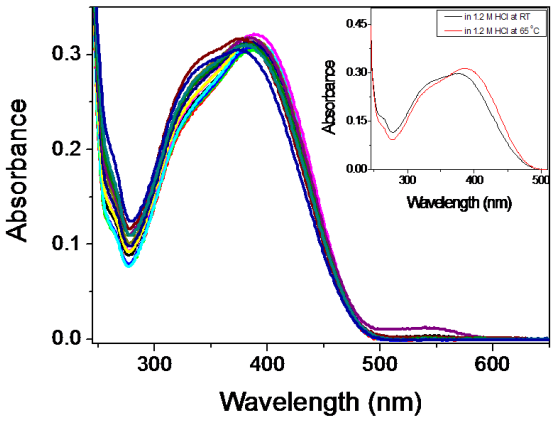

Figure S20. UV/vis apectra of **4** (3 × 10^{-5} M) equilibrated for 60 h before the experiments in different of HCl concentrations (from 0.05 M to 2.1 M) upon increasing the temperature to 65 ^{o}C.

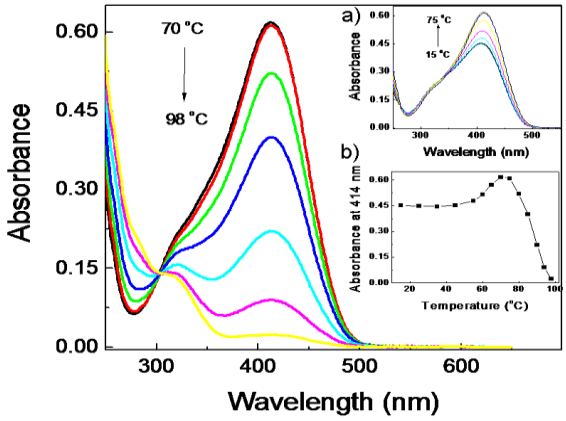

Figure S21. UV-Vis spectra of **4** (3×10^{-5} M) in water at pH 4.4 with increasing temperature from 70 °C to 98 °C. Inset a): UV-Vis spectra of **4** (3×10^{-5} M) in water at pH 4.4 with increasing temperature from 15 °C to 70 °C. Inset b): Plot of absorbance at 414 nm against temperature.

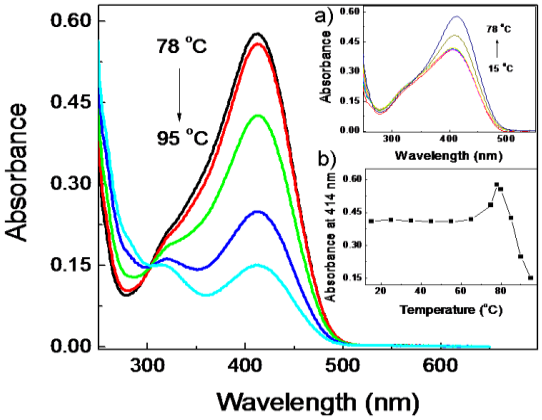

Figure S22. UV-Vis spectra of **4** (3×10^{-5} M) in water at pH 5.5 with increasing temperature from 78 °C to 95 °C. Inset a): UV-Vis spectra of **4** (3×10^{-5} M) in water at pH 5.5 with increasing temperature from 15 °C to 78 °C. Inset b): Plot of absorbance at 414 nm against temperature.

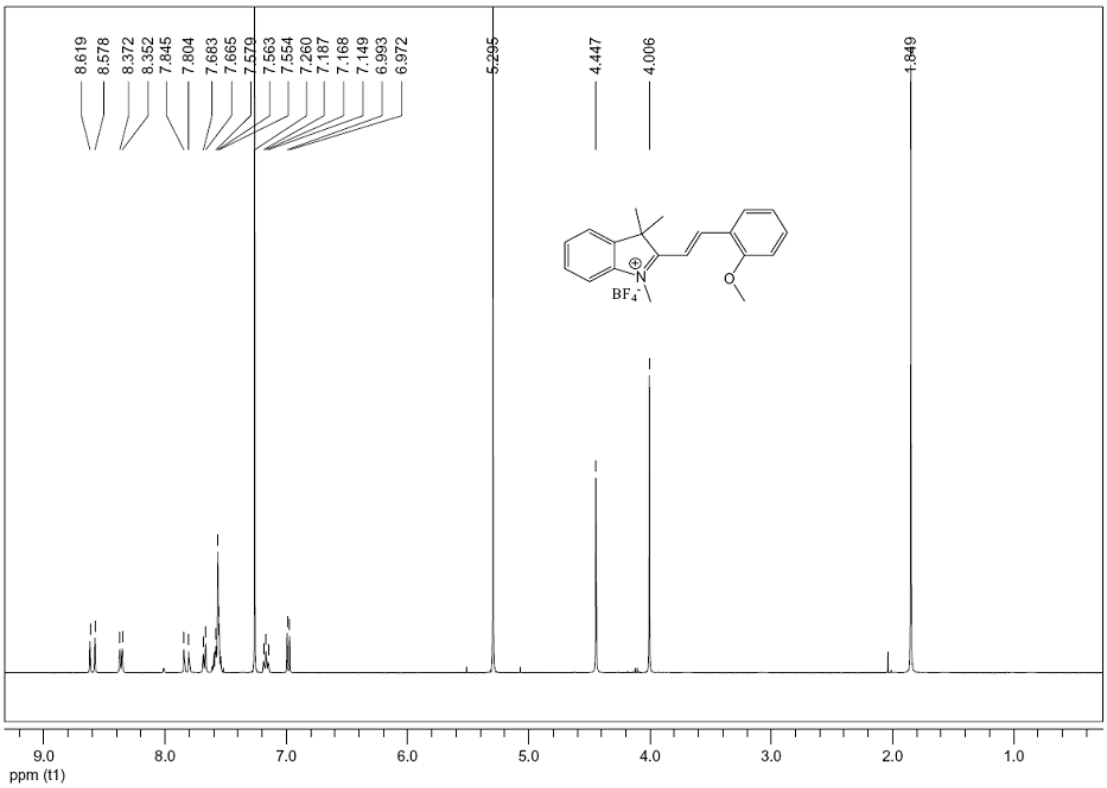

Figure S23. ^{1}H NMR of **4** (400 MHz) in $CDCl_3$.